

Synthesis and performance of star-shaped aluminum phosphinate flame retardant

Liyong Zou^{1,2} · Jiyan Liu^{1,2} · Xueqing Liu^{1,2} · Xiaomeng Wang^{1,2} · Jia Chen^{1,2}

Received: 23 July 2015 / Accepted: 22 December 2015 / Published online: 23 February 2016
© Akadémiai Kiadó, Budapest, Hungary 2016

Abstract A star-shaped aluminum dimethyl(2,2-dimethyl-1,3-propylene)bis(oxy)bicarbonylethyldiphosphate (AICP) was synthesized by esterifying reaction between 2-methyl-2,5-dioxo-1,2-oxaphospholane (OP) and neopentyl glycol following by neutralizing with aluminum hydroxide. The structure and composition were confirmed with FTIR, ¹H NMR, ³¹P NMR and X-ray fluorescent spectroscopy. AICP begins to decompose at 370 °C, matching the initial decomposition temperature of PBT. It endows PBT with desired flame retardancy and anti-dripping property and shows good compatibility with PBT. When the total filler loading is kept at 17, 15–13 mass% AICP combining with 2–4 mass% MC can make the PBT passing the UL 94 V0 rating and eliminating dripping. In addition, the AICP has a little influence on the mechanical properties of PBT. The tensile strength and notched impact strength of PBT containing 17 mass% AICP only reduce by 5.6 and 4 %, respectively, comparing to the pure PBT. The SEM photographs show that AICP has a good compatibility with PBT. Microcombustion calorimeter, TG-FTIR and SEM results show that AICP can depress the heating release and promote char forming during combustion and acts mainly in the condensed phase.

Keywords PBT · Flame retardancy · Metal phosphinate · Star-shaped phosphinate · Polyester

Introduction

The poly(butylene terephthalate) (PBT) is widely used as engineering plastic in electrical, electronic and automotive components. PBT is inherent flammability and serious dripping during combustion and involves a real hazard to the users for these applications. Hence, improving its fire resistance is very important [1, 2]. The halogen compounds are commonly used flame retardants for PBT; however, they have become under scrutiny because of ecological concerns [3, 4]. At this time, the flame retardant industry is under pressure to change to flame retardants that are perceived to be more environmentally friendly and harmless to health [5, 6].

Metal salts of phosphinate belong to a new-generation environment-friendly flame retardants. The roles of these salts in the improvement of flammability properties and in the influence of mechanical properties and the thermal stability of the composites are related to the structure of phosphinate anion and metal type of the salts [7–13]. It was found that the aluminum or calcium ethylmethylphosphinate gives V0 rating in the UL 94 test at 15 mass% loading in PBT and 20 mass% loading in glass-filled PBT, while the sodium ethylmethylphosphinate gives V0 rating at 30 mass% of filler loading in PBT [14]. In the case of aluminum salts of phosphinate-based PBT, aluminum 1-(methoxyethyl)methylphosphinate, aluminum 1-(ethoxyethyl)methylphosphinate and aluminum 1-(methoxyethyl)ethylphosphinate [15] showed only V1 rating at 20 mass% loading in glass-filled PBT. Aluminum hydroxymethylmethylphosphinate, despite of its high phosphorus content, showed only V2 rating in glass-filled

✉ Jiyan Liu
liuxueqing2000@163.com

¹ Key Laboratory of Optoelectronic Chemical Materials and Devices of Ministry of Education, Jiangnan University, Wuhan 430056, China

² Flexible Display Materials and Technology Co-innovation Center of Hubei Province, Jiangnan University, Wuhan 430056, China

PBT [16], while aluminum methylethylphosphinate or aluminum methylcyclohexylphosphinate shows V1 rating in PBT at 17 mass% filler loading. In our previous research [12, 17], influence of alkyl group of the aluminum salts of phosphinates on the properties of EP has been investigated. It was found that the metal type has more influence on the flame retardancy of the polymer, while the alkyl groups of the phosphinates affect much more the mechanical properties of the polymer and dispersion of the particles in matrix.

Commercial metal salts of phosphinates formulas for PBT are based on aluminum or zinc diethylphosphinate. However, the damage of these salts on the mechanical properties of the final materials should not be ignored. Köppl [18] investigated the effect of aluminum salts on the mechanical and thermal properties of PBT and glass fiber-reinforced PBT. For the case of PBT, 20 mass% of aluminum salts is the minimum dosage for PBT to pass the V0 rating; however, at this dosage, the tensile strength of the material is reduced by about 35 %, unnotched impact strength is reduced significantly from 190 to 20 kJ m⁻² and the elongation at break for ductility is reduced by 76 %. The deterioration of mechanical properties of the material was due to the bad dispersion of the salt particles in PBT and inferior compatibility between particle and PBT.

Balance among various properties such as thermal stability, compatibility, mechanical properties and flame retardancy is very important for high-performance flame retardants/polymer system [19, 20]. The phosphinate salts possessing the properties such as high flame retardancy, anti-dripping during combustion and good compatibility with matrix are therefore highly desired [21–24]. In addition, a highly efficient flame retardant should show a decomposition temperature similar to that of the polymer. Matching of the thermal degradation temperature between the flame retardant and polymer can make the flame retardant to act the best in both gas phase and condensed phase.

In order to improve the fire resistant efficiency and other properties of the metal salts of phosphinate-based polymer materials, adding nanoparticles or nitrogen-containing compounds such as melamine compounds has been tried [25–28]. Designing metal salts of phosphinate with appropriate structure has also been a good solution [29–31]. This article focuses on a star-shaped aluminum dimethyl(2,2-dimethyl-1,3-propylene)bis(oxy)bicarbonylethyldiphosphinate (AlCP). It was synthesized from commercial available materials 2-methy-2,5-dioxo-1,2-oxaphospholane (OP), neopentyl glycol and aluminum isopropoxide using a gentle and easy approach, as shown in Fig. 1:

Choosing neopentylglycol as reactant with OP is based on the following consideration: Polyol is often used as char

forming agent in the flame retardant system [32–34]; two hydroxyl groups in neopentyl glycol can react with OP forming a star-shaped molecule. When Al(CP) serves as a flame retardant in polymer such as PBT, the bulk organic ester group of the AlCP is expected to present high carbon forming ability and good compatibility with polymer.

Experimental

Materials

Poly(butylene terephthalate) (PBT) was obtained from Nantong Xincheng materiel Ltd. (Jiangsu, China). Melamine Cyanurate (MC) was purchased from Taixing Fine chemical Ltd. (Jinan, China). 2-Methy-2,5-dioxo-1,2-oxaphospholane (OP) with purity above 98 % was purchased by Zhenghao Chemical Ltd. (Wuhan, China). Neopentyl glycol, acetone, toluene, p-toluenesulfonic acid and aluminum isopropoxide are chemical reagents and purchased from Guoyao Chemical Ltd. (Tianjin, China) and used as received.

Synthesis of β -carboxylethylmethylphosphinic acid (CEP)

To a solution of 0.2 mol (26.8 g) OP in 100 mL of acetone was added dropwise 0.2 mol (3.60 g) water within 30 min at 50 °C. After the addition was completed, the mixture was refluxing for 2 h to obtain CEP. CEP was washed with acetone thrice and then dried at 100 °C for 24 h (yield 93 %).

Synthesis of dimethyl(2,2-dimethyl-1,3-propylene)bis(oxy)bicarbonylethyldiphosphinic acid (CP)

0.11 mol CEP (16.72 g), 0.05 mol (5.21 g) neopentyl glycol and 0.01 mol (0.17 g) p-toluenesulfonic acid were placed in a round-bottom flask equipped with a temperature controller, a reflux condenser with side arm, a nitrogen pipe and a mechanical stirrer. The mixture was heated at 120 °C under refluxing for 4 h. The white product was collected, washed with acetone (3 × 100 mL) and dried in air to obtain the CP (yield 94 %).

Synthesis of aluminum salt of dimethyl(2,2-dimethyl-1,3-propylene)bis(oxy)bicarbonylethyldiphosphinate (AlCP)

To a solution of 0.15 mol (55.8 g) CP in 200 mL of isopropanol, a solution of 0.1 mol (20.5 g) aluminum isopropoxide in 50 mL of isopropanol was added. The

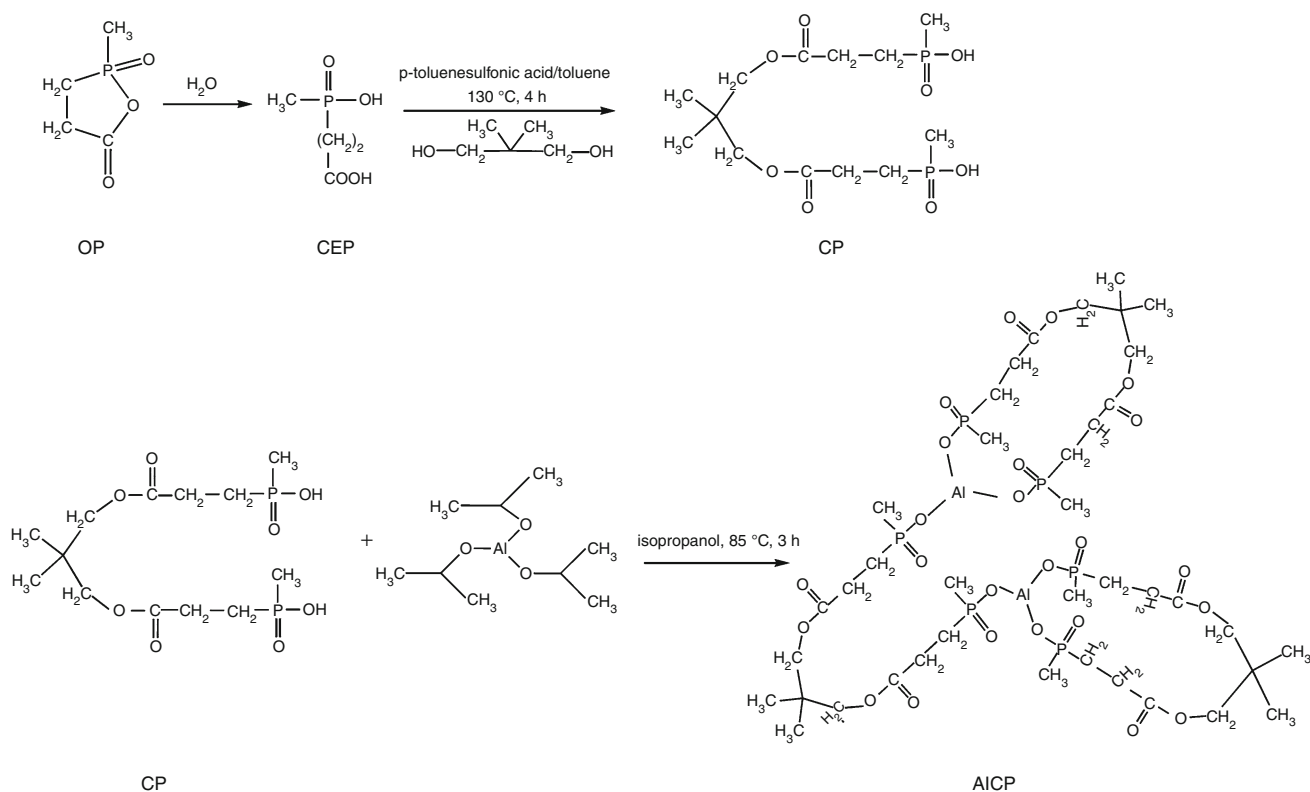


Fig. 1 Synthetic route for AICP

mixture was stirred at 85 °C under refluxing for 3 h. The crude white precipitate AICP was washed with alcohol and dried at 80 °C for 24 h (yield 96 %).

Preparation of composites

All the samples were prepared by melt blending using an XK-160 twin-screw internal mixture (Jiangsu, China) at 235 °C for 20 min with a screw speed of 120 rpm. The resulting mixture was then hot-pressed under 10 MPa at 240 °C for 5 min into sheet with suitable dimension for the further measurements. The examined formulations are listed in Table 1.

Measurements

The ¹H NMR and ³¹P NMR spectra have been recorded in a solution of DMSO-d₆ at 25 °C with a Mercury VX-300 instrument operating at 400 MHz (Varian, US), using TMS as inner reference and H₃PO₄ (85 %) as external reference. FTIR was recorded on a Tensor 27 Bruker spectrometer (Bruker, German) with KBr powder. The X-ray fluorescent spectroscopy (XRF) measurement was done with a ZSX Primus II (Rigaku, Japan) XRF spectrometer with a 35-kV Rh-anode tube. Thermogravimetric analysis (TG) was carried out with NETZSCH TG 209 thermogravimetric

Table 1 Formulation and flame retardancy of the samples

Sample	Formulation/mass%			UL94	LOI/%	Dripping
	PBT	AICP	MC			
PBT	10	0	0	–	16.6	Yes
PBT/AICP1	87	13	0	V-2	22.9	Yes
PBT/AICP/MC1	87	10.5	2.5	V-1	25.7	Yes
PBT/AICP/MC2	87	9.0	4	V-2	20.6	Yes
PBT/AICP2	83	17	0	V-1	23.5	No
PBT/AICP/MC3	83	15	2	V-0	26.8	No
PBT/AICP/MC4	83	13	4	V-0	28.3	No
PBT/AICP/MC5	83	11	6	V-0	26.4	Yes
PBT/MC	83	0	17	V-1	22.5	Yes

analyzer. Samples of about 10 mg were heated in alumina pans from room temperature up to 700 °C at a heating rate of 20 °C min⁻¹ in N₂. TG was coupled with a Nicolet iS10 FTIR spectrometer (Perkin-Elmer, USA). Limiting oxygen index (LOI) measurements were taken using a HC-2-type instrument (Jiangning, China) in accordance with ASTM D2863-77. The UL 94 vertical burning tests were conducted on a CZF-3 instrument (Jiangning, China) in accordance with ASTM D3801. The dimensions of the sample were 100 × 13 × 3 mm³. The heat release rate (HRR) and the total heat release (THR) were measured in a

MCC-2 microcombustion calorimeter (MCC) (Govmark Organization Inc., USA). Samples of about 5–7 mg were heated in alumina pans from 40 to 700 °C at a heating rate of 1 °C s⁻¹. The flow rate of N₂ and O₂ was 80 mL min⁻¹ and 20 mL min⁻¹, respectively. Samples were coated with platinum in a vacuum. Tensile property was carried out using a universal testing machine (CMT6000, SANS, Shenzhen, China) following the standard ASTM D638. The testing speed was kept at 5 mm min⁻¹. Impact testing was performed with an impact tester (ZBC1400-1, SANS, Shenzhen, China) according to standard ASTM D256 Izod Impact method. The fracture surfaces of specimens subjected to tensile were gold-coated and examined by scanning electron microscopy (SEM) using a Philips XL-40 instrument.

Results and discussion

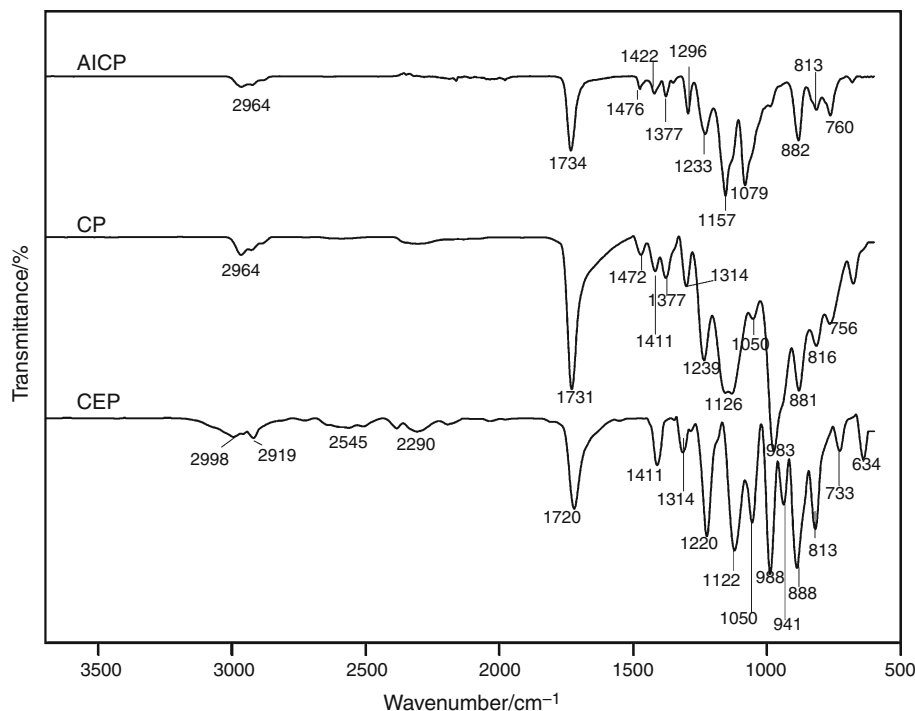
Chemical structure of AICP

Figure 2 shows the FTIR spectra of CEP, CP and AICP. In the CEP, the OH absorption of –COOH is about 3000 cm⁻¹, which overlaps with the absorption of CH₃ (2964, 2911 cm⁻¹). The broad peaks between 2700 and 2500 cm⁻¹ are attributed to the COOH. The peak at 1720 cm⁻¹ is for C=O and 1220 cm⁻¹ is for C–O in COOH. Other peaks are 1418 cm⁻¹ (CH₂), 1377 cm⁻¹ (P–CH₃), 1157 cm⁻¹ (P=O), 987 cm⁻¹ (P–O–H), 884 cm⁻¹

and 818 cm⁻¹ (CH₃) [35]. After CEP esterifying with neopentyl glycol, in the spectrum of CP, the peaks around 3000 cm⁻¹ become narrow, and peaks between 2700 and 2500 cm⁻¹ disappear; in addition, the peak for C=O of acid appearing at 1721 cm⁻¹ shifts to 1731 cm⁻¹, and peak for C–O in COOH shifts to 1235 cm⁻¹; above results indicate –COOH has taken part in the reaction and ester group was formed [36]. Other new peaks coming from neopentyl glycol are 1472 cm⁻¹ (–CH₂) and 1377 cm⁻¹ (C–(CH₃)₂) in the spectrum of CP. In the spectrum of AICP, the absorption peak at the 987 cm⁻¹ becomes weaker due to the formation of P–O–Al.

Figure 3 shows ¹H NMR and ³¹P NMR spectrum of CEP, CP and AICP. In the ¹H NMR spectrum of CEP, the shifts at 1.28, 1.32 ppm are for P–CH₃, shifts at around 1.80 ppm are for P–CH₂ and shifts at 2.36–2.43 ppm are for C–CH₂; the H in the COOH should be at 10 ppm, and the H in the POH should be at about 5–7; however, only a wide shift is observed with the peak value of 7.99 ppm. For the molecule containing both OH and COOH, only peak being observed is due to the exchange of H between OH and COOH, the location of the shift depends on intermolecular or intramolecular hydrogen [36, 37], so in the CEP, the shift at 7.93 ppm is attributed to the COOH and OH. In the ¹H NMR of CP, new shifts at 0.88–0.90 and 3.82–3.84 ppm are due to the –CH₃ and –CH₂– in neopentyl, respectively; the shift at 5.64 ppm is for the P–OH. Comparing the ¹H NMR of the AICP with CP, the shift for the POH disappears in the AICP, indicating the OH has

Fig. 2 FTIR spectra for CEP, CP and AICP



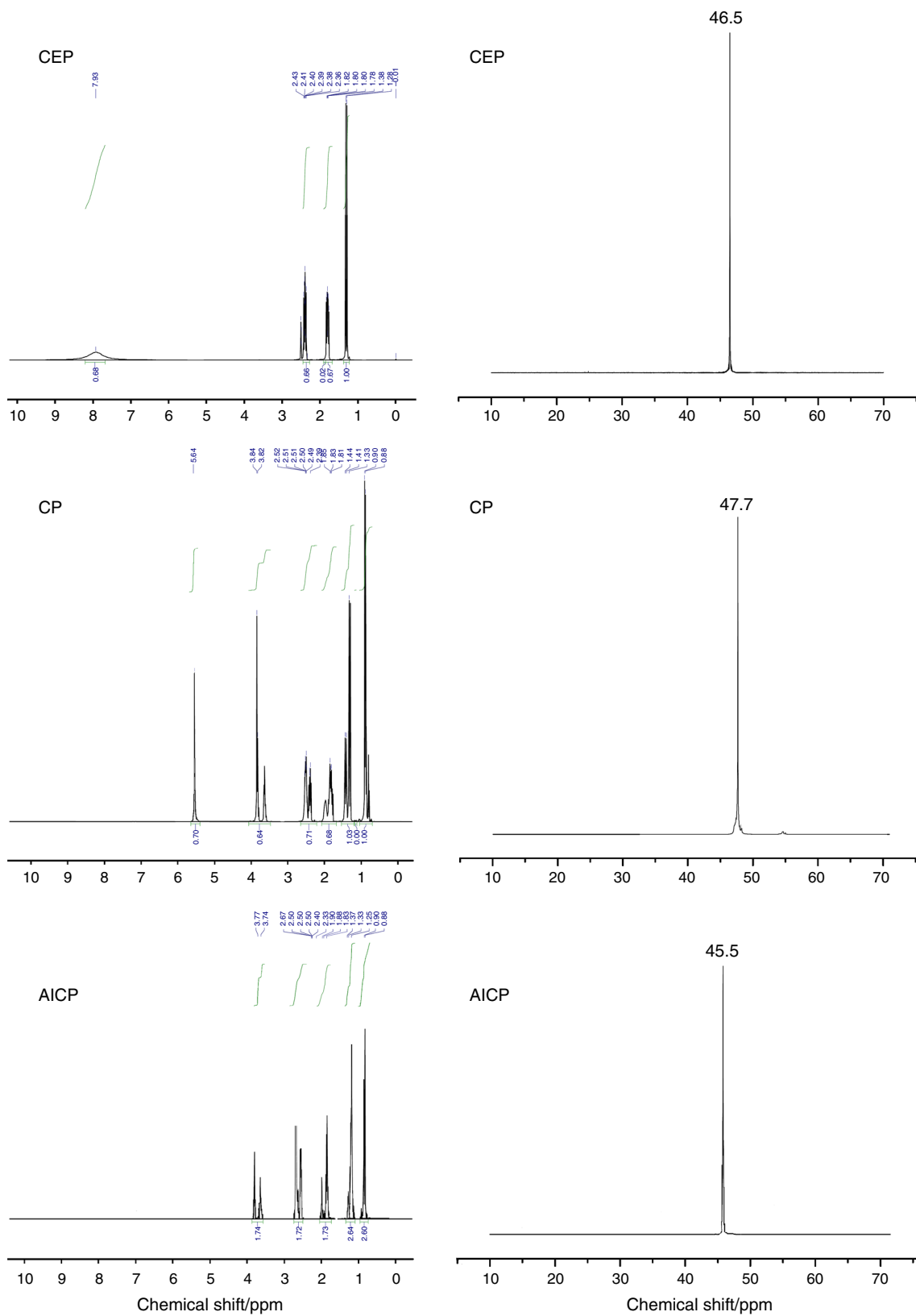


Fig. 3 ^1H NMR and ^{31}P NMR spectra for CEP and CP

formed O–Al. In the ^{31}P NMR, the shift for P of the CEP is 46.5 ppm, the shift for P of the CP is 47.7 ppm and the shift for P of the AICP is 45.5 ppm. The difference shift of the P in three substances is due to the environment of the P atom in the molecule. When CEP reacts with neopentyl glycol, forming electron-rich ester CP causes phosphorus to shift upfield. In the AICP, the Al–O–P bond shows more covalent properties and the electron density on the P atom is less than that of P–OH, so the shift for the P moves to the lower field again. This phenomenon is consistent with the explanation in the literature [37]. The XRF test shows that the Al is 3.75 mass% and the P is 12.39 mass% in the AICP; the atomic ratio of P to Al is 2.87:1, closing to the calculated value of 3:1.

The FTIR, ^1H NMR, ^{31}P NMR and the XRF data for the products are consistent with the structure as shown in Fig. 1.

Combustion characteristics: LOI, UL 94 and MCC

Table 1 reports the UL 94 test and LOI value of the samples with varying formulation. PBT is highly flammable with the LOI of 16 % and fails in the UL 94 test burning with flammable dripping. Adding 17 mass% AICP makes PBT passing the V1 rating with the LOI increasing to 23.5 % and no dripping during combustion. When the total filler loading is kept at 17 mass% and AICP is partially substituted with MC, PBT/AICP/MC3 and PBT/AICP/MC4 show satisfying flame retardancy and pass the V0 rating without dripping during combustion. PBT/AICP/MC5 passes the V0 rating but dripping during combustion. PBT/MC just passes the V1 rating with LOI of 22.5 % and dripping. Above results indicate that AICP combining with MC in an appropriate ratio shows a good flame retardancy and anti-dripping property.

PBT, PBT/AICP2 as well as the PBT/AICP/MC formulations having passed the V0 rating were further investigated with MCC. The heat release rate (HRR) curves are shown in Fig. 4, and the corresponding data such as the peak of the heat release rate (PHRR), the temperature for PHRR (T_{PHRR}), the heat release capacity (HRC) and the total heat release (THR) are presented in Table 2. Adding AICP reduces obviously the PHRR, THR and HRC of the PBT. When the AICP was partially replaced with MC, in the case of PBT/AICP/MC formulations, the T_{PHRR} and PHRR increase, whereas the HRC and THR decrease comparing to PBT/AICP2. It implies that AICP combining with MC can move the combustion of PBT to a higher temperature. The HRC is a good predictor of the flammability, and it reflects a true material property rooting in the structure and composition of the materials. Among the three PBT/AICP/MC formulations, the PBT/AICP/MC4 shows the highest T_{PHRR} and the lowest PHRR, THR and

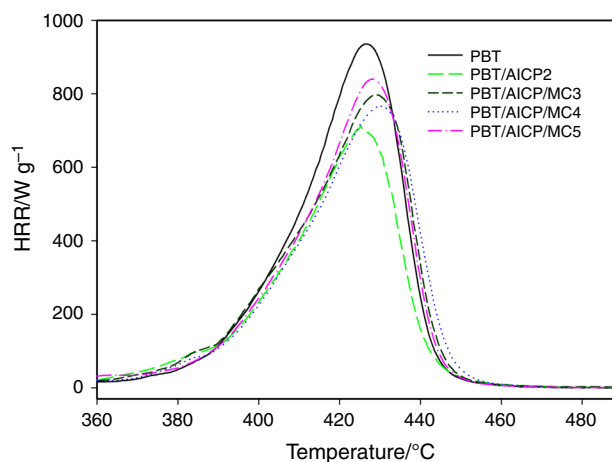


Fig. 4 HRR curves for PBT, PBT/AICP2 and PBT/AICP/MC formulations

HRC values. MCC results are consistent with the LOI and UL 94 performance.

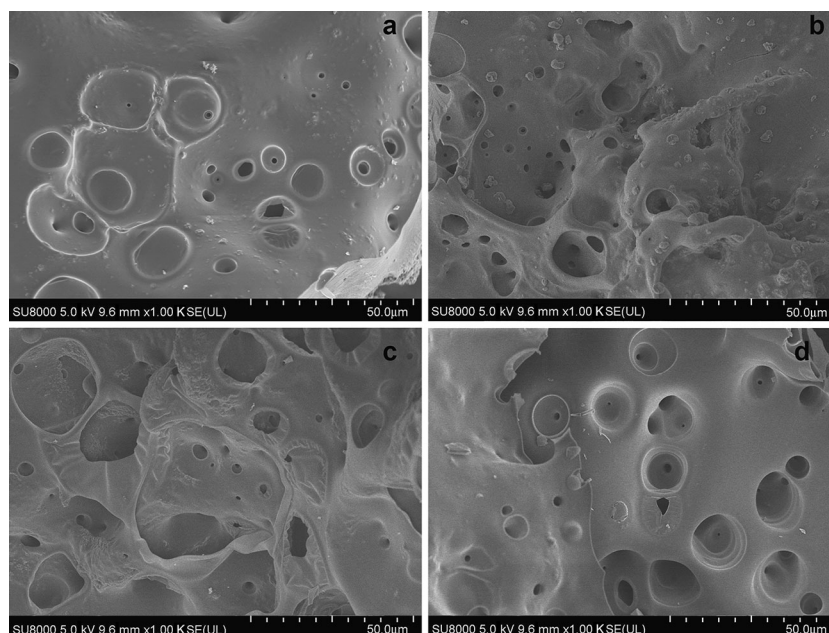
Char residues analysis

Figure 5 illustrates the SEM photographs of the char residues after combustion. The char surface of PBT/AICP2 is smooth, and a few holes of diameter less than 5 μm distribute on it. For the PBT/AICP/MC formulations, the char surface becomes rough, more and bigger holes are observed, and especially the char for PBT/AICP/MC4 has the biggest hole size. The number and the hole size on the char surface is in the order of PBT/AICP/MC4 > PBT/AICP/MC3 > PBT/AICP/MC5 > PBT/AICP2, implying the most volatile releasing from the PBT/AICP/MC4 and the least volatile coming from the PBT/AICP2 during the combustion.

The MC mainly acts in the gas phase by releasing the nonflammable gas in the PBT [35, 38]. It is supposed that the AICP acts mainly in the condensed phase by forming the dense carbonized char. For the PBT/AICP2, most of the AICP takes part in the char forming and only a little volatile produced from the AICP during the combustion; hence, the surface of the char is smooth, and a few and small holes are observed. When MC instead of the AICP is incorporated in the PBT/AICP, MC decomposes into gas coming out of the char layer and leaving lots of big holes on the surface. With the ratio of the MC/AICP increasing, the char layer becomes loose, more volatile producing from MC easily dashes out of the char layer and so bigger holes and rougher surface are observed. With the MC increasing continually, in the case of PBT/AICP/MC5, the number and the size of the holes do not increase correspondingly, and the char surface looks smoother than the char surface from PBT/AICP/MC4. Smaller hole size and smoother surface indicate less volatile dashing out of the char

Table 2 Data from MCC experiments

Samples	$T_{\text{PHRR}}/^{\circ}\text{C}$	PHRR/W g^{-1}	THR/ kJ g^{-1}	HRC/J $\text{g}^{-1} \text{K}^{-1}$
PBT	426 \pm 2	889 \pm 14	23.3 \pm 0.1	661 \pm 10
PBT/AICP2	425 \pm 3	706 \pm 16	19.0 \pm 0.2	533 \pm 20
PBT/AICP/MC3	428 \pm 2	795 \pm 11	19.4 \pm 0.2	557 \pm 14
PBT/AICP/MC4	430 \pm 2	762 \pm 18	19.3 \pm 0.1	547 \pm 17
PBT/AICP/MC5	427 \pm 3	838 \pm 20	19.9 \pm 0.2	589 \pm 19

**Fig. 5** SEM results for **a** PBT/AICP2, **b** PBT/AICP/MC3, **c** PBT/AICP/MC4 and **d** PBT/AICP/MC5 after burning

surface. In order to investigate this phenomenon, FTIR coupling with thermal degradation analysis was used to monitor the volatile releasing.

Thermal degradation analysis

Figure 6 shows the TG-DTG curves of samples with different formulation in N_2 . Detailed and precise parameters including the temperature at 5 % mass loss ($T_{5\%}$), the maximum rate degradation temperature (T_{max}), the maximum decomposition rate (DTG_{max}) and the char yields at 700 °C are summarized in Table 3. AICP shows good thermal stability with the $T_{5\%}$ 368 °C, and the char at 700 °C is 35.3 %. Adding AICP reduces the $T_{5\%}$ and DTG_{max} of PBT slightly, and the char residues of PBT are

improved. When the total filler loading is kept at 17 mass%, the AICP is partially replaced with MC, the $T_{5\%}$, T_{max} and char at 700 °C of the PBT/AICP/MC formulations are reduced comparing with PBT/AICP. During being heated, the MC decomposed into gas, and most of the AICP forms the char residues remaining in the condensed phase. Theoretically, the char yield should reduce with MC increasing. However, TG results show that the PBT/AICP/MC4 has the lowest char yield among the three PBT/AICP/MC formulations. The probable reason is following: MC decomposes earlier than AICP, at higher MC content, the lots of nonflammable gas release from the MC before the decomposition of the matrix and AICP, this nonflammable gas depressed decomposition of the components in formulation, some of the components that did not decompose

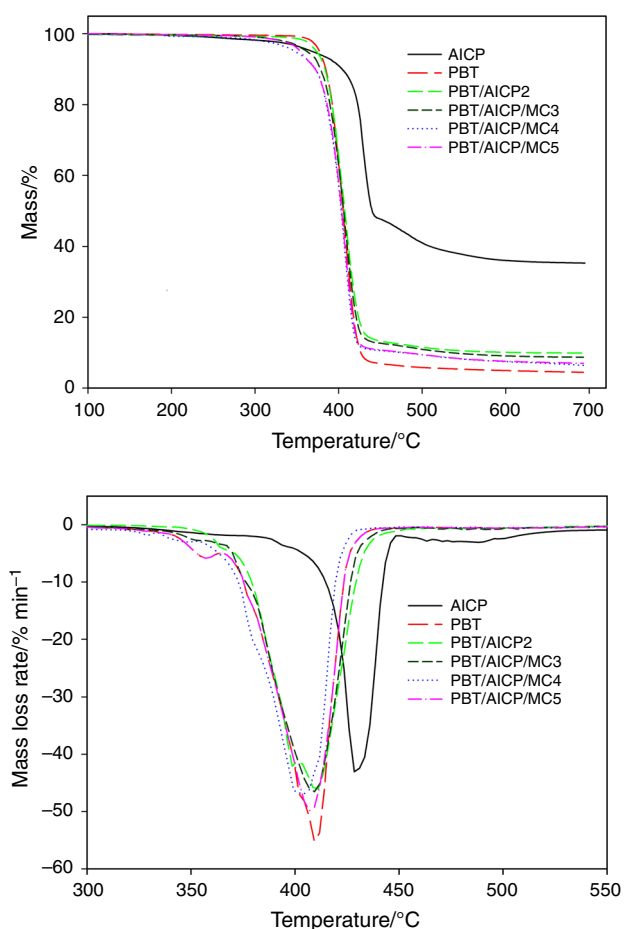


Fig. 6 TG-DTG curves for the samples in N_2

Table 3 TG-DTG data for the samples in N_2

Sample	T_5 %/°C	T_{max} /°C	DTG _{max} / % min ⁻¹	Char at 700 °C/%
AICP	369	430	42.9	35.3
PBT	377	410	55.2	4.4
PBT/AICP2	374	411	46.0	9.9
PBT/AICP/MC3	362	410	46.6	8.7
PBT/AICP/MC4	347	403	46.8	6.4
PBT/AICP/MC5	354	408	49.7	7.0

then were trapped by the char, so the char yield increases again in the PBT/AICP/MC5.

FTIR analysis for volatilized products

Figure 7 presents the intensity of total volatile with time for the various formulations. The area under the curve is the total intensity of the peaks; it can be obtained by integrating the curve. The pure PBT starts releasing volatile after 17 min, and one peak is observed with the area of the peaks

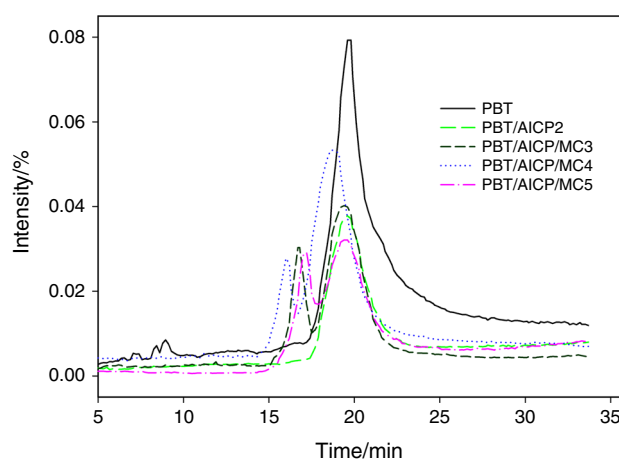


Fig. 7 Intensity of the total pyrolysis gas for the samples at different times

0.4714. Adding AICP into PBT reduces the intensity of the volatile greatly, and the total area of the peaks for the PBT/AICP2 is 0.2373. After the AICP was partially replaced with MC, for the PBT/AICP/MC formulations, the peak of the volatile becomes wider and two peaks are observed. The MC starts to decompose at about 310 °C, so the first peak is mainly contributed by the MC, and the second peak is contributed by all the components in the formulation. In addition, the peaks for the PBT/AICP/MC4 appear earlier and the total area of the peaks (0.3607) is larger than that of PBT/AICP/MC3(0.2380) or PBT/AICP/MC5 (0.2487), indicating PBT/AICP/MC4 has lower decomposition temperature and produces more volatile than PBT/AICP/MC3 and PBT/AICP/MC5, which agrees with the SEM observation in Fig. 5 that lots of gas releasing from the sample lead to the large holes in the char surface of PBT/AICP/MC4.

FTIR spectra for the volatile coming from the various formulations at 17, 19 and 22 min are presented in Fig. 8. At 17 min, the temperature is about 380 °C, the pure PBT just starts degrading and almost no signal is detected. When the AICP is added into PBT, signals for the volatile coming from PBT in the case of PBT/AICP2 can be detected as following: 3730 and 3587 cm^{-1} (benzoic acid), 3587 cm^{-1} (water), 3038 cm^{-1} (benzene), 2970 and 1021 cm^{-1} (tetrahydrofuran THF) 2350 and 617 cm^{-1} (CO_2), 1741, 1268 and 1108 cm^{-1} (ester), 915 cm^{-1} (butadiene) and 734 cm^{-1} (C–H in aromatic ring) [8, 12]. For the PBT/AICP/MC formulations, the signals at 2350 and 2380 cm^{-1} become intense and a new signal for the HOCN deriving from the MC is observed at 2252 cm^{-1} . CO_2 and HOCN are main products during degradation of MC [19]; of course they are higher in concentration in PBT/AICP/MC than in PBT or PBT/AICP. At 19 min, the PBT reaches the maximum degradation rate; strong signals for the volatile from neat PBT can be observed. Adding AICP into PBT leads that all signals relating to PBT become

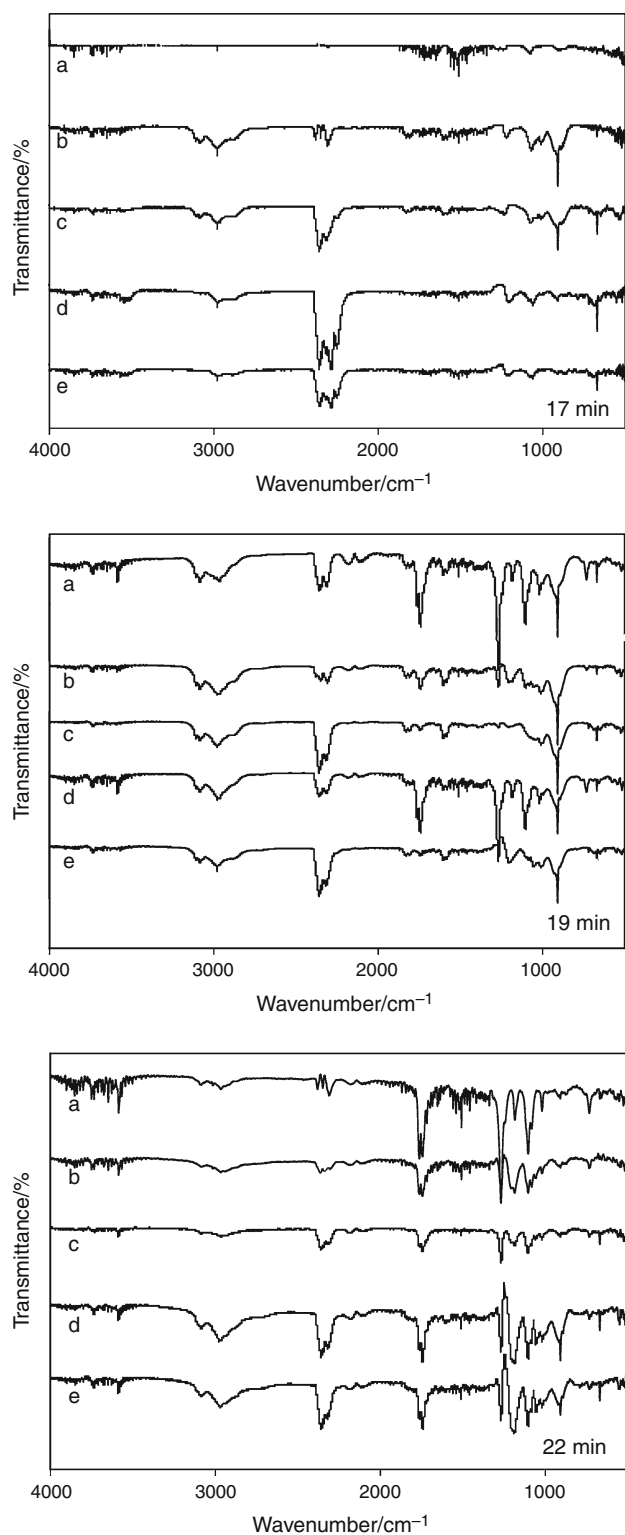


Fig. 8 FTIR spectra of pyrolysis products for *a* PBT, *b* PBT/AICP2, *c* PBT/AICP/MC3, *d* PBT/AICP/MC4, *e* PBT/AICP/MC5 at different times

weak except signals at 2970 and 3080 cm^{-1} , where the signals of THF overlap with the signals of CH_2 from the AICP. At 22 min, new signals at the 1200, 1049 and

Table 4 Mechanical properties of the samples

Sample	$\varepsilon_x/\%$	E/MPa	TS/MPa	$\text{NIS}/\text{kJ m}^{-2}$
PBT	19.6 ± 1.1	494 ± 8	53 ± 9	6.0 ± 0.2
PBT/AICP1	17.1 ± 1.5	514 ± 9	52 ± 12	5.8 ± 0.3
PBT/AICP/MC1	16.2 ± 1.7	523 ± 10	50 ± 8	5.7 ± 0.4
PBT/AICP/MC2	15.6 ± 1.6	509 ± 11	48 ± 10	5.6 ± 0.3
PBT/AICP2	15.2 ± 1.3	536 ± 9	50 ± 11	5.8 ± 0.4
PBT/AICP/MC3	15.4 ± 1.4	506 ± 10	50 ± 11	5.5 ± 0.2
PBT/AICP/MC4	14.9 ± 1.6	514 ± 12	50 ± 12	5.4 ± 0.3
PBT/AICP/MC5	14.5 ± 1.4	522 ± 13	49 ± 8	5.3 ± 0.2
PBT/MC	14.3 ± 1.2	533 ± 11	49 ± 10	5.1 ± 0.1

1015 cm^{-1} due to the P=O and P-O of the AICP are observed in the formulations containing AICP.

TG-FTIR results show that adding AICP leads the PBT to decompose faster in the early stage and then depress the degradation of the PBT at higher temperature, which is similar to the function of aluminum methylcyclohexylphosphonates [30]. On the other hand, the volatile coming from the AICP is detected at higher temperature and the signals are weaker than those producing by PBT and MC, indicating most of AICP was left in the condensed phase to prevent the PBT from degradation.

MC mainly acts in the gas phase by releasing the non-flammable gas diluting the flammable substance [39, 40]. Appropriate combination of AICP and MC can make the flame retardants acting in the gas and the condensed phase simultaneously and shows optimum synergistic effect by forming loose char layer to isolate the heat and flammable gas from the inner layer of the materials. Combining flammable test and MCC determination indicates that the PBT/AICP/MC4 shows the satisfying flame retardancy and anti-dripping properties during combustion. SEM photographs and TG-FTIR measurement show that PBT/AICP/MC4 formed the loose char layer and released more volatile than the other two PBT/AICP/MC formulations. It needs a further investigation in the future why the formulation with specific combination shows the better synergism than others.

Mechanical properties

The tensile properties including elongation at breaking ($\varepsilon\%$), tensile strength (TS), tensile modulus (E) and notched impact strength (NIS) are summarized in Table 4. Adding AICP into PBT reduces the $\varepsilon\%$, TS and NIS of the PBT, but the E is increased. The reduction in above-mentioned parameters is far less than the diethylphosphinate-filled PBT [18]. For the PBT/AICP2, the ε_x , TS and NIS values are lower by 22, 5.6 and 4 %, respectively, than pure PBT. When the AICP is partially replaced with MC, the mechanical properties of the samples almost have no change.

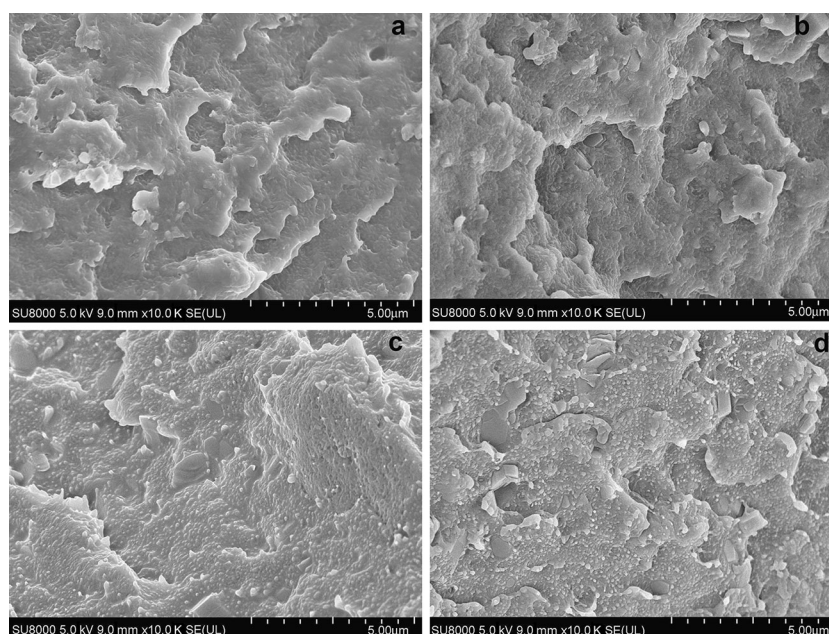


Fig. 9 SEM results for fracture surface of **a** PBT/AICP2, **b** PBT/AICP/MC3, **c** PBT/AICP/MC4 and **d** PBT/AICP/MC5 before burning

Figure 9 presents the SEM photographs for the fracture surface of the samples. Almost no naked particles are seen on the surface, indicating a good compatibility between PBT and AICP. Good compatibility is probably due to the bulk ester-containing organic group in the AICP, which has a similar structure and polarity to the PBT.

Conclusions

Star-shaped aluminum phosphinates AICP was successfully synthesized. The synthesis process and the products were characterized by the FTIR, NMR and XRF. AICP is endowed with good thermal stability, desired flame retardancy, anti-dripping property as well as good dispersion in PBT. The AICP begins to decompose at 370 °C in nitrogen, matching the initial decomposition temperature of PBT very well. Similar decomposition temperature between the flame retardant and polymer can make the flame retardant to play a maximum role in both gas phase and condensed phase during polymer combustion.

Adding 17 mass% AICP alone in PBT can make the PBT reaching the UL94 V1 rating and eliminating dripping. TG-FTIR results showed that the AICP catalyzes the decomposition of the PBT at the early decomposition stage and promotes char forming at higher temperature. And more importantly, the AICP has a little influence on the mechanical properties of the PBT. The tensile strength and notched impact strength of the PBT containing 17 mass% AICP only reduce by 5.6 and 4 %, respectively, comparing with the pure PBT. The SEM photographs show that AICP has a good compatibility with PBT.

When the total filler loading is kept at 17, 13–14 mass% AICP combining with 2–4 mass% MC can make the PBT passing the V0 rating and eliminating dripping. In the PBT/AICP/MC formulations, PBT/AICP/MC4 containing 4 mass% MC and 13 mass% AICP shows the best flame retardancy and lowest heat release during combustion. SEM photographs show that the char from the PBT/AICP/MC4 is looser and rougher than other PBT/AICP/MC formulations. The reasons why the components in PBT/AICP/MC4 have a maximum synergistic effect need to investigate in the future work.

Acknowledgements This work is supported by of the academic innovation program for the outstanding youth groups of universities in Hubei (T201318) and key project of nature science founding of Hubei (2014CFA098).

References

1. Levchik SV, Weil ED. A review on thermal decomposition and combustion of thermoplastic polyesters. *Polym Adv Technol.* 2004;15:691–700.
2. Levchik SV, Weil ED. Flame retardancy of thermoplastic polyesters—a review of the recent literature. *Polym Int.* 2005;54:11–35.
3. Veen IV, Boer J. Phosphorus flame retardants: properties, production, environmental occurrence, toxicity and analysis. *Chemosphere.* 2012;88:1119–53.
4. Ramani A, Dahoe AE. On the performance and mechanism of brominated and halogen free flame retardants in formulations of glass fiber reinforced poly(butylene terephthalate). *Polym Degrad Stab.* 2014;104:71–86.
5. Balabanovich AI, Engelmann J. Fire retardant and charring effect of poly(sulfonyldiphenylene phenylphosphonate) in poly(butylene terephthalate). *Polym Degrad Stab.* 2003;79:85–92.

6. Gallo E, Braun U, ScharTEL B, Russo P, Acierno D. Halogen-free flame retarded poly(butylene terephthalate) (PBT) using metal oxides/PBT nanocomposites in combination with aluminum phosphinate. *Polym Degrad Stab.* 2009;94:1245–53.
7. Balabanovich AI. Thermal decomposition study of intumescent additives: pentaerythritol phosphate and its blend with melamine phosphate. *Thermochim Acta.* 2005;435:188–96.
8. Balabanovich AI. The effect of ammonium polyphosphate on the combustion and thermal decomposition behavior of poly(butylene terephthalate). *J Fire Sci.* 2003;21:285–98.
9. Höerold S. Flame-retarding thermosetting compositions. US Patent 6,420,459 (2002).
10. Stanley R, Springfield S. Polyester resins flame retarded by poly(metal phosphinates)s. US Patent 4,180,495 (1979).
11. Brehme S, Koeppl T, ScharTEL B, et al. Competition in aluminium phosphinate-based halogen-free flame retardancy of poly(butylene terephthalate) and its glass-fibre composites. *E-Polymer.* 2014;14(3):729–47.
12. Braun U, Bahr H, Sturm H, ScharTEL B. Flame retardancy mechanisms of metal phosphinates and metal phosphinates in combination with melamine cyanurate in glass-fiber reinforced poly(1,4-butylene terephthalate): the influence of metal cation. *Polym Adv Technol.* 2008;19:680–92.
13. Liu XQ, Liu JY, Cai SJ. Comparative study of aluminum diethylphosphinate and aluminum methylethylphosphinate-filled epoxy flame-retardant composites. *Polym Compos.* 2012;33:918–26.
14. Kleiner HJ, Budzinsky W. Flame proofed polyester molding composition. US Patent 6,013,707 (2000).
15. Kleiner H, Jenewein El, Wanzke, W. Alkyl-1-alkoxyethylphosphinous acid aluminium salts. EP 971,936 (2002).
16. Kleiner H. Aluminium salts of alkylhydroxymethylphosphinic acids. US Patent 6,303,674 (2001).
17. Liu XQ, Liu JY, You QL, He D, Guo YH, Cakmak M. Influence of structure of metal salts of phosphinates on the performance of flame-retardant polymer. In: 30th International conference of the polymer processing society (PPS-30). Cleveland, OH, USA; 2014.
18. Köppl T, Brehme S, Wolff-Fabris F. Structure-property relationships of halogen-free flame-retarded poly(butylenes terephthalate) and glass fiber reinforced PBT. *J Appl Polym Sci.* 2012;124:9–18.
19. Yang H, Song L, Tai Q, Wang X, Yu B, Hua Y, Yuen RK. Comparative study on the flame retarded efficiency of melamine phosphate, melamine phosphite and melamine. *Polym Degrad Stab.* 2014;105:248–56.
20. Brehme S, ScharTEL B, Goebbels J, Fischer O, Pospiech D, Bykov Y, Döring M. Phosphorus polyester versus aluminium phosphinate in poly(butylene terephthalate) (PBT): flame retardancy performance and mechanisms. *Polym Degrad Stab.* 2011;96:875–84.
21. Brehme S, Köppl T, ScharTEL B, Fischer O, Altstädt V, Pospiech D, Döring M. Phosphorus polyester—an alternative to low-molecular-weight flame retardants in poly(butylene terephthalate)? *Macromol Chem Phys.* 2012;213:2386–97.
22. Köppl T, Brehme S, Pospiech D. Influence of polymeric flame retardants based on phosphorus-containing polyesters on morphology and material characteristics of poly(butylene terephthalate). *J Appl Polym Sci.* 2013;128:3315–24.
23. Wang X, Song L, Yang H, Lu H, Hu Y. Synergistic effect of graphene on antidripping and fire resistance of intumescent flame retardant poly(butylene succinate) composites. *Ind Eng Chem Res.* 2011;50:5376–83.
24. Doğan M, Erdoğan S, Bayraml E. Mechanical, thermal, and fire retardant properties of poly(ethylene terephthalate) fiber containing zinc phosphinate and organo-modified clay. *J Therm Anal Calorim.* 2013;112:871–6.
25. Braun U, ScharTEL B. Flame retardancy mechanisms of aluminium phosphinate in combination with melamine cyanurate in glass-fibre reinforced poly(1,4-butylene terephthalate). *Macromol Mater Eng.* 2008;293:206–17.
26. Naik AD, Fontaine G, Samyn F, et al. Melamine integrated metal phosphates as non-halogenated flame retardants: Synergism with aluminium phosphinate for flame retardancy in glass fiber reinforced polyamide 66. *Polym Degrad Stab.* 2013;98:2653–62.
27. Isitman NA, Kaynak C. Nanoclay and carbon nanotubes as potential synergists of an organophosphorus flame-retardant in poly (methyl methacrylate). *Polym Degrad Stab.* 2010;95:1523–32.
28. Isitman NA, Dogan M, Bayramli E, Kaynak C. The role of nanoparticle geometry in flame retardancy of polylactide nanocomposites containing aluminium phosphinate. *Polym Degrad Stab.* 2012;97:1285–96.
29. Bauer H, Höerold S, Krause W. Salts of alkyl esters of carboxyethyl(alkyl)phosphinic acid. US Patent 7,838,580 B2 (2010).
30. Liu XQ, Liu JY, Chen J, Cai SJ, Hu CL. Novel flame-retardant epoxy composites containing aluminium b-carboxylethylmethylphosphinate. *Polym Eng Sci.* 2015;55:657–63.
31. Liu JY, Chen J, Liu XQ. Synthesis of aluminium methylcyclohexylphosphinate and its use as flame retardant for epoxy resin. *Fire Mater.* 2014;38:155–65.
32. Wang Z, Lv P, Hu Y, Hu K. Thermal degradation study of intumescent flame retardants by TG and FTIR: melamine phosphate and its mixture with pentaerythritol. *J Anal Appl Pyrol.* 2009;86:207–14.
33. Chen YH, Wang Q. Reaction of melamine phosphate with pentaerythritol and its products for flame retardation of polypropylene. *Polym Adv Technol.* 2007;18:587–600.
34. Lv P, Wang Z, Hu K, et al. Flammability and thermal degradation of flame retarded polypropylene composites containing melamine phosphate and pentaerythritol derivatives. *Polym Degrad Stab.* 2005;90:523–34.
35. Yang W, Lu H, Tai Q, Qiao Z, Hu Y, Song L, Yuen RK. Flame retardancy mechanisms of poly(1,4-butylene terephthalate) containing microencapsulated ammonium polyphosphate and melamine cyanurate. *Polym Adv Technol.* 2011;22:2136–44.
36. Odinets IL, Antonov EA, Petrovsky PV, Morozik YuI, Krivolapov YuA, et al. Interaction of 2-methyl-2,5-dioxo-1,2-oxaphospholane with trimethylsilyl cyanide. *Russ Chem Bull.* 1994;43(1):121–4.
37. Williams D, Fleming I. *Spectroscopic methods in organic chemistry.* New York: McGraw Hill; 2007.
38. Balabanovich AI. The effect of melamine on the combustion and thermal decomposition behaviour of poly(butylene terephthalate). *Polym Degrad Stab.* 2004;84:451–8.
39. Nagasaw Y, Ozaw HK. Fast thermolysis/FT-IR studies of fire-retardant melamine-cyanurate and melamine-cyanurate containing polymer. *J Anal Appl Pyrol.* 1995;33:253–67.
40. Sangeetha V, Kanagathara N, Sumathi R, Anbalagan G. Spectral and thermal degradation of melamine cyanurate. *J Mater.* 2013;2013:1–7.